Journal of Alloys and Compounds 523 (2012) 75–82

Contents lists available at SciVerse ScienceDirect

Journal of Alloys and Compounds

journal homepage: www.elsevier.com/locate/jallcom

Homogeneity range and crystal structure of the $Ca_2Mg_5Zn_{13}$ compound

Yi-Nan Zhang[a], Dmytro Kevorkov[a], Xue Dong Liu[b], Florent Bridier[c], Patrice Chartrand[d], Mamoun Medraj[a,*]

[a] Department of Mechanical Engineering, Concordia University, 1455 de Maisonneuve Blvd. W., Montreal, Quebec, Canada, H3G 1M8
[b] Center for the Physics of Materials and the Department of Physics, McGill University, 3600 University Street, Montreal, Quebec, Canada, H3A 2T8
[c] Department of Mechanical Engineering, École de Technologie Supérieure, 1100 Notre-Dame Ouest, Montreal, Quebec, Canada, H3C 1K3
[d] Center for Research in Computational Thermochemistry École Polytechnique (Université de Montréal), Montreal, Quebec, Canada, H3C 3A7

ARTICLE INFO

Article history:
Received 29 October 2011
Received in revised form 7 January 2012
Accepted 12 January 2012
Available online 1 February 2012

Keywords:
Intermetallics
Phase identification
Diffraction
Electron microprobe
Electron microscopy

ABSTRACT

The homogeneity range and crystal structure of the $Ca_2Mg_5Zn_{13}$ ternary solid solution were determined using SEM, EPMA, EBSD, TEM and X-ray diffraction. This compound has the $Ca_xMg_yZn_z$ ($8.2 \le x \le 9.1$; $27.1 \le y \le 31.0$; $60.8 \le z \le 64.7$) composition range at 335 °C. The refinement of the XRD patterns was carried out by Rietveld analysis. XRD data showed that this solid solution crystallizes in a hexagonal structure having $P6_3/mmc$ (194) space group and $Sm_3Mg_{13}Zn_{30}$ prototype. The well indexed SAED patterns and Kikuchi diffraction pattern obtained from TEM and EBSD confirmed the crystallographic information obtained by XRD. The atomic coordination spheres and site occupancy were determined. On the basis of the atomic occupancy results and the crystallographic details, a three-sublattice model is proposed for this compound.

1. Introduction

The growing need for lightweight, energy-efficient, "green" environmentally friendly products is driving the development of magnesium-based alloys. Such development is mainly realized through a combination of innovative structural design and promising alloys for energy generation, energy storage and transportation [1,2]. The addition of Ca and Zn elements in Mg alloys enhances the strength, castability, creep and corrosion resistance, fracture toughness and age hardening response [3,4]. Recently the biocompatible glassy alloys with a small amount of Ca have been found in the Ca–Mg–Zn ternary system for the development of biodegradable implants [5–8]. These biodegradable metallic implants can be designed to stabilize structure by allowing bone to grow while simultaneously dissolving harmlessly in the body and thereby reducing the burden of surgical intervention [5,7,8]. Hence the Ca–Mg–Zn system is promising as a next-generation material in both transportation and biomedical applications. Understanding the phase equilibria and crystal structure of the ternary intermetallic compounds is necessary for further development of alloys in this system and for better understanding of the existing ones. To date, many researchers have studied the $Ca_2Mg_6Zn_3$ compound, but their results are contradictory [9–14]. More recently, the solubility range and crystal structure of a Mg-rich solid solution were determined using scanning electron microscopy (SEM), electron probe micro-analysis (EPMA), transmission electron microscopy (TEM) and X-ray diffraction (XRD) by our group [15,16]. In addition, another ternary compound $Ca_2Mg_5Zn_{13}$ with solubility ranges and its XRD pattern were reported by Clark [10,17], but the crystallographic information was not reported in terms of lattice parameters, space group and structure type. Therefore, the purpose of the present research is to investigate the homogeneity range and crystal structure of the $Ca_2Mg_5Zn_{13}$ ternary compound in the Ca–Mg–Zn system. To be consistent with our previous paper [16], $Ca_2Mg_5Zn_{13}$ ternary solid solution is addressed as IM3 (intermetallic compound) in this paper.

2. Experimental procedure

Three solid–solid diffusion couples and four key alloys were prepared. The starting materials were Mg (purity 99.98%), Zn (99.99%) ingots and Ca (99%) supplied by Alfa Aesar. The key alloys were prepared in an arc-melting furnace with water-cooled copper crucible in an argon atmosphere using a non-consumable tungsten electrode. Samples were remelted five times to ensure homogeneity. The actual composition of the samples was determined by inductively coupled plasma-mass spectrometry (ICP-MS). The difference between nominal compositions and actual compositions is below 3 at.%. To prepare solid–solid diffusion couples, the contacting surfaces were ground down to 1200 grit SiC paper and polished using 1 μm water-based diamond suspension with 99% pure ethanol as a lubricant. Two end members were carefully pressed, clamped with a steel ring, placed in a Ta container and sealed in a quartz tube. The tube was filled with argon to avoid the reaction

* Corresponding author.
E-mail address: mmedraj@encs.concordia.ca (M. Medraj).

0925-8388/$ – see front matter © 2012 Elsevier B.V. All rights reserved.
doi:10.1016/j.jallcom.2012.01.068

Table 1
The actual composition of the key samples, phases present and the compositions of IM3 ternary compound.

Sample No.	Actual composition identified by ICP (at.%)			Phases identification	Composition of IM3 identified by EPMA			IM3 phase composition identified by Rietveld analysis (statistical distribution of atoms in the crystallographic positions)		
	Ca	Mg	Zn	By EPMA	Ca	Mg	Zn	Ca	Mg	Zn
1	7.5	48.3	44.2	Mg IM3	8.8	30.1	61.1	8.7	28.4	62.9
2	4.6	40.1	55.3	IM3 IM4 $Mg_{12}Zn_{13}$	8.2	31.0	60.8	8.0	30.7	61.3
3	4.7	25.2	70.1	IM3 $MgZn_2$ $CaZn_{11}$ $CaZn_{13}$	8.2	27.1	64.7	8.1	27.3	64.6
4	15.2	22.6	62.2	IM1 IM2 IM3	9.1	27.4	63.5	8.7	27.7	63.6

Table 2
Refined crystal structure parameters of other phases for KS1 and KS3.

Samples No.	Phase	Prototype	Space group	Lattice parameters		
				a (Å)	*b* (Å)	*c* (Å)
KS1	Mg	Mg	$P6_3/mmc$ (194)	3.198 (2)	3.198 (2)	5.197 (4)
	$MgZn_2$	$MgZn_2$	$P6_3/mmc$ (194)	5.222 (1)	5.222 (1)	8.568 (6)
KS3	$CaZn_{11}$	$BaCd_{11}$	$I4_1/amd$ (141)	10.796 (8)	10.796 (8)	6.871 (9)
	$CaZn_{13}$	$NaZn_{13}$	*Fm*-3*c* (194)	12.172 (2)	12.172 (2)	12.172 (2)

Table 3
1st case: crystal structure of the IM3 phase in KS1 without statistical distribution of atoms in the crystallographic position.

IM3 phase composition by EPMA	$Ca_{8.8}Mg_{30.1}Zn_{61.1}$					
IM3 phase composition identified by Rietveld analysis	$Ca_{8.7}Mg_{28.3}Zn_{63.0}$					
Prototype	$Sm_3Mg_{13}Zn_{30}$					
Space group	$P6_3/mmc$ (194)					
Unit cell parameters and lattice volume	Atomic coordinates (Wyckoff position)	Atomic positions			B_{iso}	Reliability factors[a]
		x	*y*	*z*		
a = 14.760 (3) Å *c* = 8.806 (4) Å *V* = 1661.38 (6) Å^3	Ca1 – 6h	0.456 (6)	0.904 (2)	0.25	1.179 (4)	R_e = 11.81
	Ca2 – 2a	0	0	0	1.179(4)	R_{wp} = 14.08
	Mg1 – 12k	0.117 (3)	0.236 (2)	0.559 (2)	1.100(3)	*s* = 1.42
	Mg1 – 12k	0.232 (5)	0.457 (2)	0.056 (2)	1.100(3)	
	Mg3 – 2d	0.3333	0.6667	0.75	1.100(3)	
	Zn1 – 12k	0.568 (3)	0.127 (1)	0.083 (1)	1.109(6)	
	Zn2 – 12j	0.065 (5)	0.303 (5)	0.25	1.109(6)	
	Zn3 – 12j	0.409 (6)	0.120 (6)	0.25	1.109(6)	
	Zn4 – 12i	0.358 (4)	0	0	1.109(6)	
	Zn5 – 4f	0.3333	0.6667	0.100 (1)	1.109(6)	
	Zn6 – 6h	0.074 (1)	0.120 (1)	0.25	1.109(6)	

[a] Reliability factors: *s* presents the goodness of fit; R_{wp} is the weighted summation of residuals of the least squared fit; R_e is the value statistically expected.

of Mg and Ca with air. Samples were annealed at 335 °C for 4 weeks followed by quenching in water. The terminal compositions of the solid–solid diffusion couples along with the key samples are shown in Fig. 1.

The microstructure, layer thickness, phase composition, and homogeneity ranges were analyzed using quantitative EPMA (JEOL-JXA-8900) with a 2 μm probe diameter, 15 kV accelerating voltage, 20 nA probe current. Phi–Rho–Z (PRZ) matrix corrections (modified ZAF) were applied during the analysis. The error of the EPMA measurements was estimated to be about ±2 at.%. This value was obtained using statistical analysis of the compositions of selected phases from several samples. XRD was used for phase analysis and determination of the solubility limits. The XRD patterns were obtained using PANalytical X'pert Pro powder X-ray diffractometer with a Cu Kα radiation at 45 kV and 40 mA. The XRD spectrum was acquired from 20° to 120° 2θ with a 0.02° step size. The analysis of the X-ray patterns was carried out using X'Pert HighScore Plus Rietveld analysis software in combination with Pearson's crystal database [18]. To improve the surface condition for electron

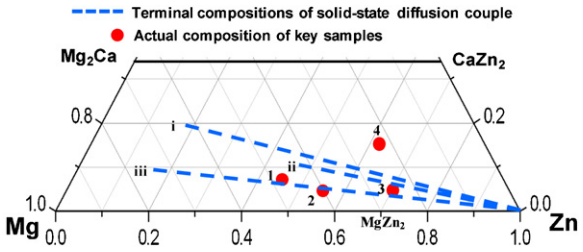

Fig. 1. The composition of the samples and diffusion couples used to determine the homogeneity range and crystal structure of the $Ca_2Mg_5Zn_{13}$ (IM3) ternary compound.

Table 4
2nd case: crystal structure of the IM3 phase in KS1 with statistical distribution of atoms in the crystallographic position.

IM3 composition by EPMA	$Ca_{8.8}Mg_{30.1}Zn_{61.1}$						
IM3 phase composition identified by Rietveld analysis	$Ca_{8.7}Mg_{28.4}Zn_{62.9}$						
Prototype	$Sm_3Mg_{13}Zn_{30}$						
Space group	$P6_3/mmc$ (194)						
Unit cell parameters and lattice volume	Atomic coordinates (Wyckoff Position)	Occupancy (%)	Atomic positions			B_{iso}	Reliability factors
			x	*y*	*z*		
a = 14.756 (3) Å	Ca1 – 6h	Ca 100	0.456 (4)	0.909 (4)	0.25	5.704(5)	R_e = 11.81
c = 8.804 (4) Å	Mg1 – 12k	Mg 100	0.119 (3)	0.240 (3)	0.565 (2)	0.271 (2)	R_{wp} = 13.71
V = 1660.153 (5) Å^3	Mg2 – 12k	Mg 100	0.236 (4)	0.455 (5)	0.055 (3)	0.271(2)	*s* = 1.35
	Zn1 – 12k	Zn 100	0.568(6)	0.127(3)	0.085(2)	2.860(3)	
	Zn2 – 12j	Zn 100	0.066(4)	0.3034	0.25	2.860(3)	
	Zn3 – 12j	Zn 100	0.408(3)	0.119(3)	0.25	2.860(3)	
	Zn4 – 12i	Zn 100	0.360(3)	0	0	2.860(3)	
	Zn5 – 4f	Zn 100	0.3333	0.6667	0.100(3)		
	Zn6 – 2a	Zn 100	0	0	0	2.860(3)	
	Ca,Mg1 – 2d	Ca 100, Mg 0	0.3333	0.6667	0.75	5.704(5)	
	Mg,Zn1 – 6h	Mg 35, Zn 65	0.067(4)	0.120(3)	0.25	0.271(2)	

Table 5
Selected atomic bond lengths of the IM3 compound in KS 1.

Atom1	Atom2	Distance (Å)
Ca,Mg1	Zn1	3.082 (1)
Mg2	Zn1	2.883 (2)
Ca,Mg1	Zn5	3.082 (1)
Mg2	Zn5	2.719 (3)
Mg2	Mg2	3.467 (2)
Mg2	Mg1	3.045 (2)
Mg,Zn1	Mg,Zn1	2.710 (1)
Mg,Zn1	Zn2	2.653 (3)
Mg,Zn1	Zn6	2.700 (1)

back-scattered diffraction (EBSD) measurements, the samples were first subjected to a standard mechanical metallographic procedure, then cleaned with plasma, ion milled, and again cleaned with plasma. EBSD analysis was performed using a Hitachi SU-70 Schottky-SEM equipped with a Nordlys F+ camera and Oxford HKL Channel 5 software. Typical operation parameters were a 20 kV accelerating voltage and a 13 nA beam current. Phases were identified by comparing experimental Kikuchi diffraction patterns with patterns computer-generated from the crystallographic information of identified structure. Ternary key sample $Ca_{6.2}Mg_{48.3}Zn_{45.5}$ was prepared to study the crystal structure of IM3 compound by TEM. The sample was crushed using a mortar and pestle and the fragments were suspended in ethanol before depositing them on a carbon coated Cu grid. The selected area electron diffraction (SAED) and Philips CM200 TEM operated at 200 kV were used to analyze the IM3 compound.

Table 7
Comparison of lattice parameters of the IM3 measured by XRD and TEM.

Lattice parameters of IM3	
a (Å)	*c* (Å)
14.758 (XRD)	8.804 (XRD)
14.93 (TEM)	8.86 (TEM)

3. Results and discussion

The homogeneity ranges and crystal structure of IM3 solid solution were studied by EPMA, XRD, EBSD and TEM using diffusion couples and key samples.

3.1. Determination of homogeneity ranges by diffusion couples and key samples

To determine the phase boundaries of the IM3 ternary phase, three diffusion couples and four ternary samples were prepared and studied. Their micrographs are illustrated in Fig. 2. The homogeneity limits of IM3 solid solution were studied by EPMA and XRD. The actual compositions, the identified phases and the compositions of IM3 are summarized in Table 1. The actual chemical compositions of these alloys were determined by ICP. The phase analysis was carried out using XRD and EPMA. The phase

Table 6
Refined crystal structure parameters of the IM3 solid solutions and atomic coordinates for Ca,Mg1 – 2d and Mg,Zn1-2h positions for KS1-4.

Samples no.	Lattice parameters			Atomic coordinates (Wyckoff Position)	Occupancy (%)	Reliability factors		
	a (Å)	*c* (Å)	*V* (Å^3)			R_e	R_{wp}	*s*
1	14.756 (3)	8.804 (4)	1660.123(5)	Ca,Mg1 – 2d Mg,Zn1 – 6h	Ca 100, Mg 0 Mg 35, Zn 65	11.8	13.7	1.35
2	14.744 (3)	8.752 (4)	1647.700(5)	Ca,Mg1 – 2d Mg,Zn1 – 6h	Ca 70, Mg 0 Mg 60, Zn 40	11.3	22.3	3.87
3	14.734 (4)	8.760 (4)	1647.575(5)	Ca,Mg1 – 2d Mg,Zn1 – 6h	Ca 73, Mg 0 Mg 10, Zn 90	10.3	20.1	3.78
4	14.747 (4)	8.814 (5)	1659.940(6)	Ca,Mg1 – 2d Mg,Zn1 – 6h	Ca 100 Mg 0 Mg 25, Zn 75	11.0	21.6	3.84

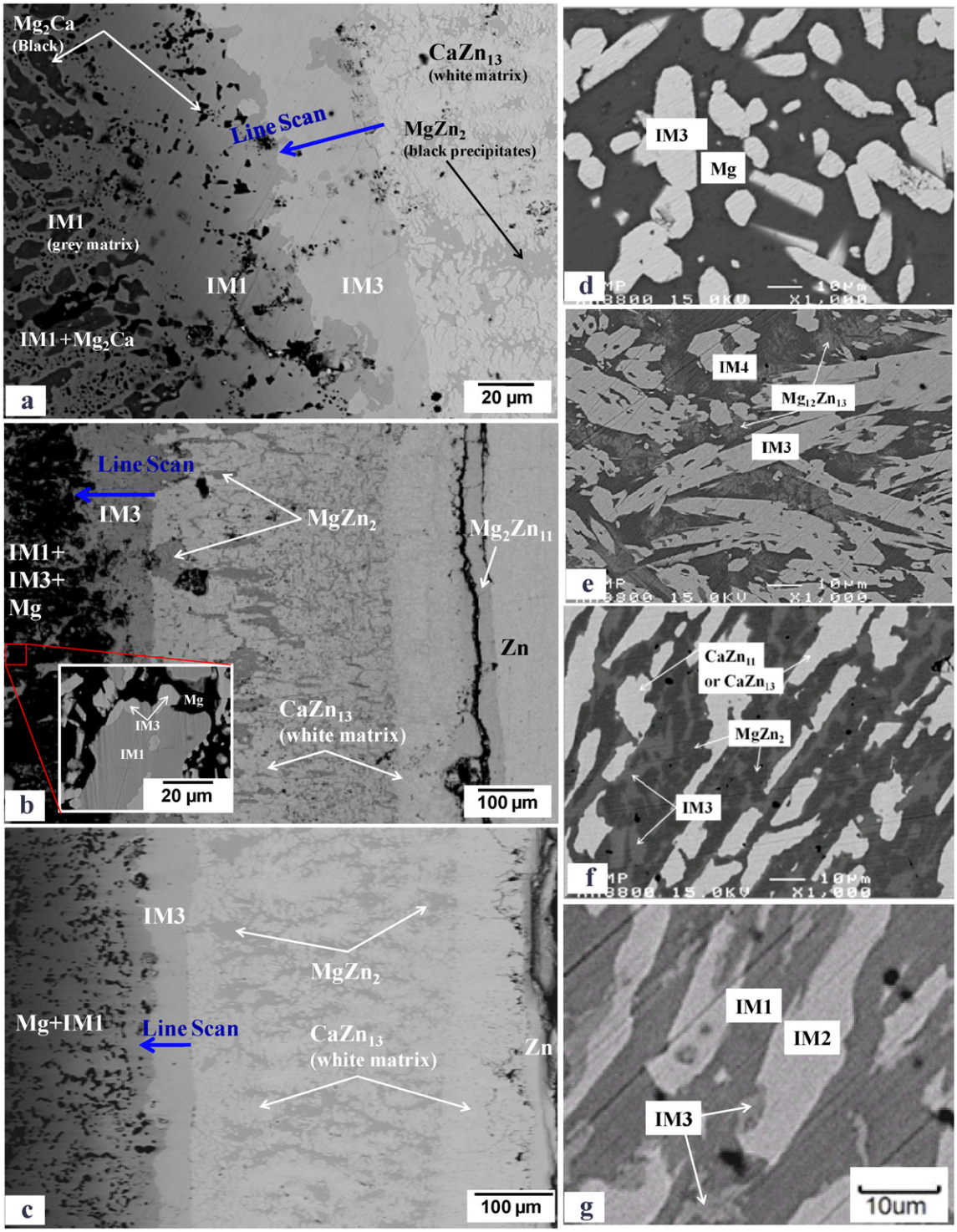

Fig. 2. BSE images: (a) DC1, (b) DC2, (c) DC3, (d) KS1, (e) KS2, (f) KS3 and (g) KS4. All samples are annealed at 335 °C for 4 weeks.

boundaries of the IM3 phase were determined by EPMA and confirmed by XRD (Rietveld analysis). During heat treatment, extensive interdiffusion of Ca, Mg and Zn took place in the diffusion couples allowing various equilibrium phases to form. EPMA line scans were used to determine the solubility ranges of the IM3 ternary solid solution, as shown in Fig. 2(a)–(c). The phase compositions in key samples were studied by EPMA point analysis. To determine the phase boundaries of IM3 ternary phase, four ternary samples KS 1–4 were prepared to identify the solid solubility limits, as illustrated in Fig. 1. BSE image of these samples annealed at 335 °C for 4 weeks are shown in Fig. 2(d)–(g). The phase relations obtained from EPMA are consistent with the XRD results. As could be seen in Table 1, the compositions of the IM3 solid solution determined by EPMA and obtained from Rietveld analysis of XRD patterns are in good agreement with one another.

The solubility range of the IM3 solid solution is obtained from the analysis of all the EPMA results from the solid–solid diffusion couples and the key alloys. This compound has a complex homogeneity range of 8.2–9.1 at.% Ca, 27.1–31.0 at.% Mg and 60.8–64.7 at.% Zn. Partial isothermal section of the Ca–Mg–Zn

Table 8
Comparison of planar space (d value ($h\,k\,l$)) of the IM3 measured by XRD and TEM.

($h\,k\,l$)	d (Å) (KS1)	
	From SAED	By XRD
1 0 1	7.31	7.250
2 0 1	5.23	5.172
3 0 0	4.31	4.260
2 1 1	4.30	4.235
5 0 0	2.56	2.556
2 1 3	2.51	2.508
3 3 0	2.49	2.460
3 1 3	2.27	2.260
5 1 1	2.24	2.221
5 2 1	1.98	1.993
3 0 4	1.97	1.955

system at 335 °C with the phase boundaries of IM3 ternary solid solution along its phase relations is illustrated in Fig. 3. To understand the nature of such complex solubility a detailed crystallographic study was performed, which will be discussed below. The composition of the IM3 solid solution is close to the composition of the ω phase reported by Clark [10] as approximately 8.4–10.1 at.% Ca, 25.7–28.5 at.% Mg and 61.4–65.9 at.% Zn.

3.2. Determination of crystallographic information for IM3 compound

X-ray powder diffraction was used to obtain the X-ray pattern of the IM3 phase. XRD patterns of KS1 and KS3 annealed at 335 °C for 4 weeks are presented in Fig. 4(a) and (b), respectively. The XRD patterns of IM3 phase have shown a good agreement with the one reported by Clark [17]. However, Clark did not identify the crystal structure. Only the experimental XRD pattern was reported. The XRD pattern of KS1 was indexed using Treor software included in X'Pert HighScore Plus package combined with Pearson's crystallographic database [18]. It was found that IM3 compound crystallizes in the $Sm_3Mg_{13}Zn_{30}$ prototype [19] with hexagonal structure and $P6_3/mmc$ (194) space group. Full pattern refinement was carried out by the Rietveld method. The use of Si as an internal calibration standard enabled correcting the zero shift and specimen surface displacement. Since KS1 and KS3 samples are not single phase alloys, the refinement of IM3 phase was made in combination with other phases. The crystallographic data for these phases were taken from the Pearson's database. The refined lattice parameters of these phases are shown in Table 2.

The pattern of the KS1 sample was used for Rietveld analysis of the IM3 compound. First, the crystal structure was refined without statistical distribution of elements in the atomic positions. The results of refinement are presented in Table 3. Since the IM3 phase has a wide homogeneity range the statistical distribution of

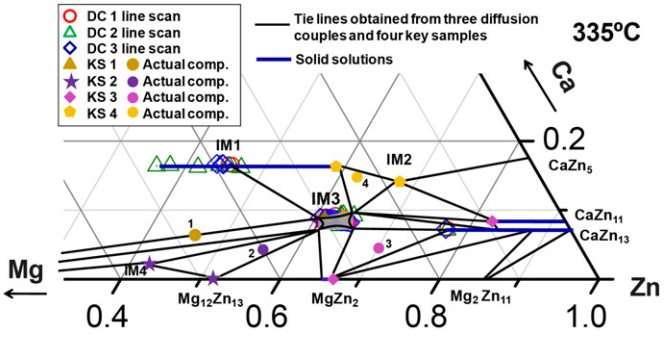

Fig. 3. Partial isothermal section of the Ca–Mg–Zn system at 335 °C showing the phase relations and solubility limits of IM3 ternary solid solution.

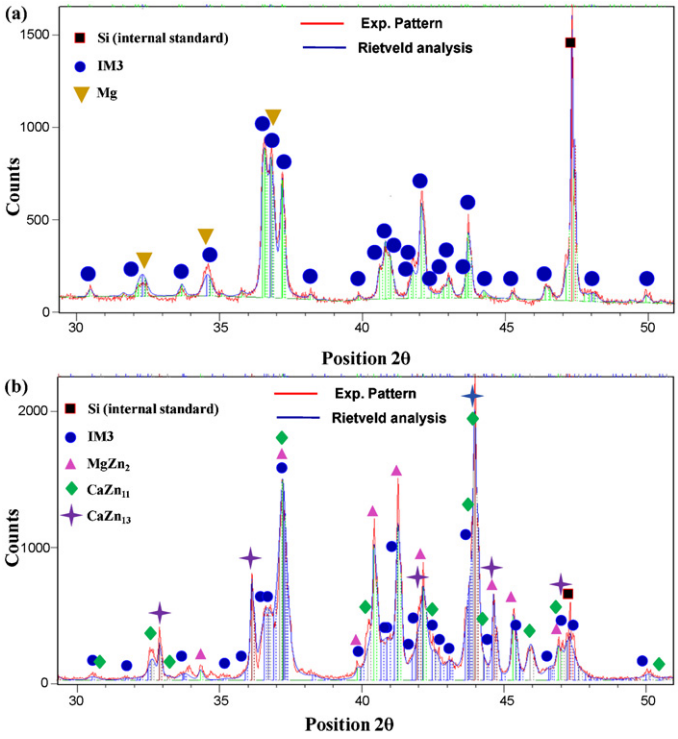

Fig. 4. Rietveld analysis: (a) KS 1, (b) KS 3. Both are annealed at 335 °C for 4 weeks.

elements in the atomic positions was implemented to the model. The crystallographic parameters of the refinement are presented in Table 4.

The composition of IM3 obtained from Rietveld analysis is consistent with the corresponding EPMA results in both cases. In the first case (Table 3), Zn atoms are substituted by Ca atoms completely at 2a sites. Whereas in the second case (Table 4), the 2d (for Ca,Mg1) and 6h (for Mg,Zn1) positions were used for statistical distribution of atoms. These positions were selected because the analysis of interatomic distances allowed to accommodate the atoms with bigger size. As can be seen in Table 5, most of bond lengths with Ca,Mg1 (2d atomic coordinates) and Mg,Zn1 (6h atomic coordinates) demonstrate relatively larger distances, indicating that the Mg in Ca,Mg1 and Zn in Mg,Zn1 have higher potential to be substituted by Ca and Mg, respectively. In addition, the statistically expected values R_e, weighted summation of residuals of the least squared fit R_{wp} and goodness of fit s were used to judge the degree of refinement in the Rietveld analysis. It is apparent that the 2nd case has better reliability factors.

Table 6 shows the refined structural parameters of IM3 and the reliability factors for all four key samples. The atomic coordinates and site occupancy for Ca,Mg1 – 2d and Mg,Zn1 – 2h positions were studied. The coordination spheres and atomic substitution of Mg by Ca at 2d sites and Zn by Mg at 6h sites as well as other sites were identified and presented in Fig. 5.

3.3. Crystallographic information obtained by TEM and EBSD

The structure of the IM3 compound (KS1) was also studied by TEM. According to the crystallographic data of IM3 obtained by XRD, the hexagonal structure was indexed and confirmed by means of SAED data, as shown in Fig. 6(a) and (b). The lattice parameters a and c as well as the planar spacing, d values, obtained from the SAED pattern of KS1 show good consistency with the XRD results, as can be seen in Tables 7 and 8. In addition, the consistent results of d and ($h\,k\,l$) values (Table 8) as well as the lattice parameters a

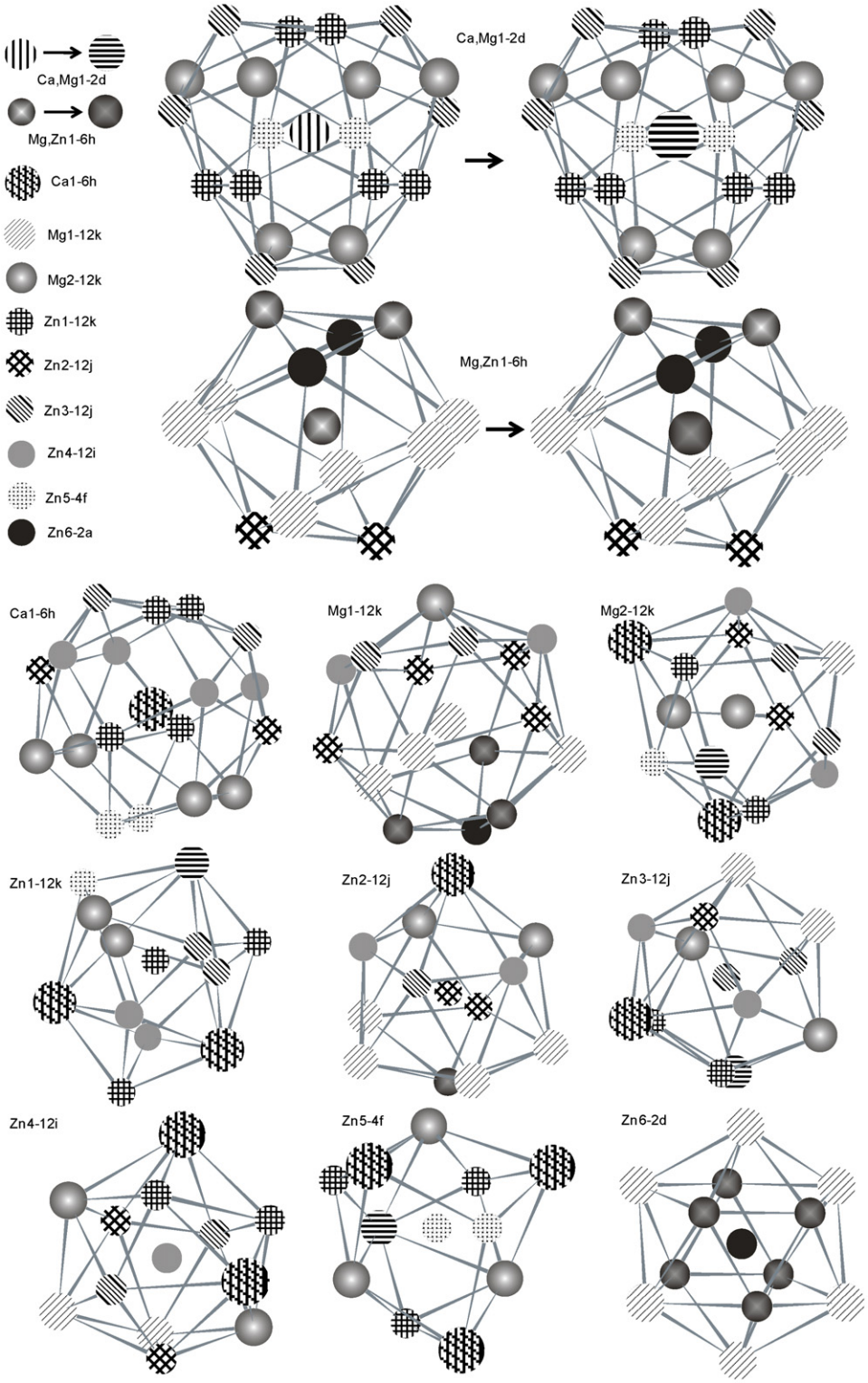

Fig. 5. The coordination spheres of atomic substitution at 2d for (Ca,Mg) and 6h for (Mg,Zn) and other positions.

and *c* (Table 7) obtained from XRD and SAED patterns support the fact that this ternary phase has the provided hexagonal structure. Hence the space group and lattice parameters obtained by XRD are confirmed by TEM. EBSD analysis was also carried out to confirm the crystallographic information of IM3 ternary compound and the Kikuchi diffraction pattern was studied. The well indexed Kikuchi diffraction pattern confirms correct selection of space group, prototype and correct values for the lattice parameters obtained from XRD and TEM, as shown in Fig. 6(c) and (d). The left side is unindexed EBSD pattern and the right side is indexed one for IM3 ternary compounds.

Furthermore, modeling of the intermetallic solid solution requires information regarding the crystal structure of the phases and their homogeneity ranges. From the crystallographic data obtained in this work, the following sublattice model is applied to represent the current compound:

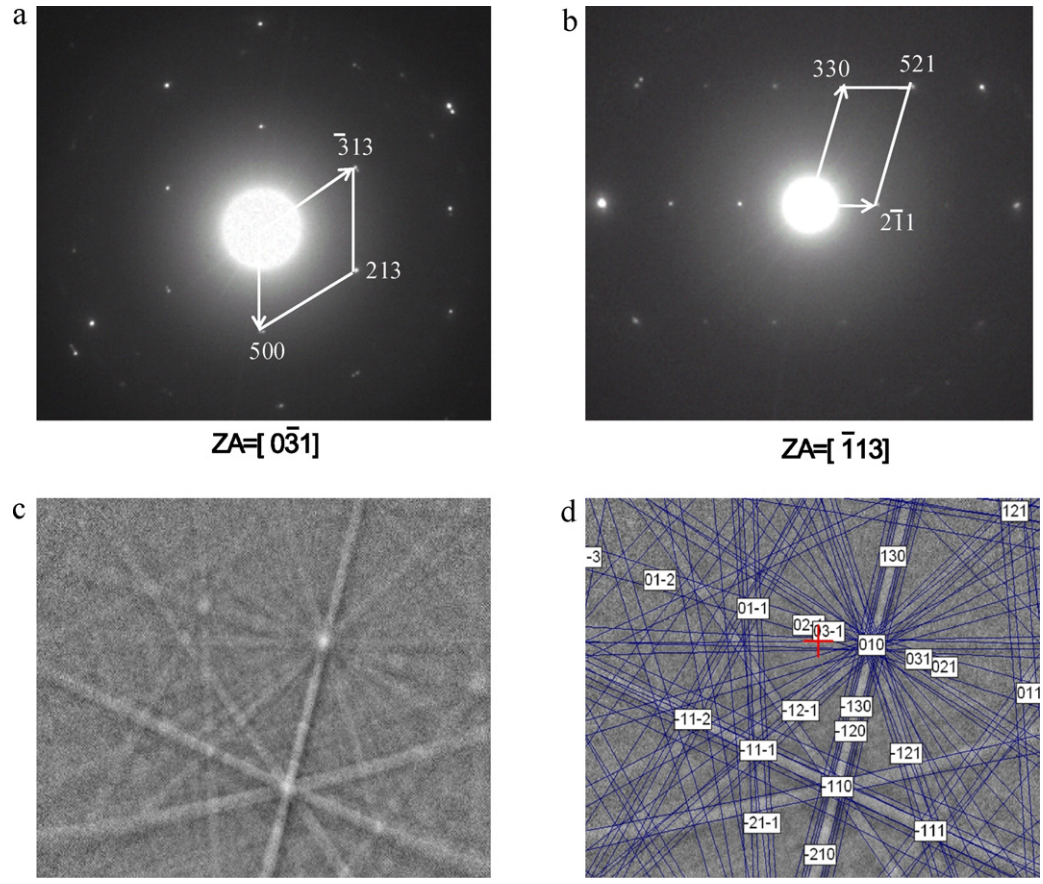

Fig. 6. (a) SAED pattern of IM3 [1 $\bar{3}$ 1] zone axis indexed as a hexagonal structure; (b) SAED pattern of IM3 [1 1 3] zone axis indexed as a hexagonal structure; (c) un-indexed and (d) indexed EBSD pattern for IM3 ternary compound.

$(Ca)_6(Mg)_{12}(Mg)_{12}(Zn)_{12}(Zn)_{12}(Zn)_{12}(Zn)_{12}(Zn)_4(Zn)_2$

$(Ca, Mg\%)_2(Mg, Zn\%)_6$ (Model I).

Here the '%' denotes the major constituent of the sublattice.

According to Kumar and Wollants [20] the number of sublattices can be reduced by grouping sublattices together with similar crystallographic characteristics such as same coordination number and or same symmetry, where Zn at Zn1-12k, Zn2-12j, Zn3-12j and Zn4-12i coordinate sites are the same coordination numbers (equal to 12) as well as Mg at Mg1-12k and Mg2-12k are the same symmetry, Zn1, Zn2, Zn3 and Zn4 as well as Mg1 and Mg2 sites should be coupled respectively to reduce the number of end members. The sublattice model can be written as:

$(Ca)_6(Mg)_{24}(Zn)_{48}(Zn)_4(Zn)_2(Ca, Mg\%)_2(Mg, Zn\%)_6$ (Model II).

Model II can be simplified further with grouping the same atoms in one sublattice. The sublattice model for this compound can be presented:

$(Ca)_3(Mg)_{12}(Zn)_{27}(Ca, Mg\%)(Mg, Zn\%)_3$ (Model III).

This five-sublattice model provides a solubility range of $6.5 \le Ca \le 8.7$ at.%, $26.1 \le Mg \le 34.8$ at.% and $58.7 \le Zn \le 65.2$ at.%, which almost covers the homogeneity range of the $Ca_xMg_yZn_z$ ($8.2 \le x \le 9.1$; $27.1 \le y \le 31.0$; $60.8 \le z \le 64.7$ at 335 °C) compound.

In reality, in order to have a more practical sublattice model suitable for thermodynamic modeling of this compound, some sublattices should be allowed to mix and extend the homogeneity range. In addition, to be consistent with the formula of prototype $Sm_3Mg_{13}Zn_{30}$, the final model can be finalized to:

$(Ca)_3(Ca, Mg\%)_{13}(Mg, Zn\%)_{30}$ (Model IV).

This three-sublattice model covers a solubility range of $6.5 \le Ca \le 34.9$ at.%, $0 \le Mg \le 93.5$ at.% and $0 \le Zn \le 65.2$ at.%, which covers the homogeneity range of above suggested five-sublattice model and the IM3 ternary compound.

4. Conclusion

The compositions and homogeneity range of the $Ca_2Mg_5Zn_{13}$ (IM3) ternary phase in the Ca–Mg–Zn system were determined. This compound has the $Ca_xMg_yZn_z$ ($8.2 \le x \le 9.1$; $27.1 \le y \le 31.0$; $60.8 \le z \le 64.7$) solid solubility region at 335 °C. The refinement of the XRD patterns was carried out by Rietveld analysis. It has hexagonal structure with $P6_3/mmc$ (194) space group and $Sm_3Mg_{13}Zn_{30}$ prototype. The atomic coordinates and site occupancy were determined. The positions of 2d for (Ca,Mg1) and 6h for (Mg,Zn1) are in favor of substitution of Mg by Ca and Zn by Mg, respectively. Selected area electron diffraction TEM data and the planar spacing d values obtained by Rietveld analysis demonstrate excellent consistency. The crystallographic information obtained by XRD is confirmed by TEM and EBSD. Combining the atomic occupancy results and the crystallographic details obtained in this work, a three-sublattice $(Ca)_3(Ca,Mg\%)_{13}(Mg,Zn\%)_{30}$ model is suggested for this compound.

Acknowledgments

Financial support from General Motors of Canada Ltd. and NSERC through the CRD grant program is gratefully acknowledged. The authors would like to thank Ming Wei and Alain Tessier from the Chemistry Department of Concordia University for their help in conducting the ICP-MS measurements. The authors would also like to thank Pierre Hovington from Hydro-Quebec research center for his help in sample preparation for EBSD analysis.

References

[1] T.M. Pollock, Science 328 (5981) (2010) 986–987, doi:10.1126/science.1182848.
[2] A.A. Luo, International Materials Review 49 (1) (2004) 13–30.
[3] M. Aljarrah, M. Medraj, X. Wang, E. Essadiqi, G. Dénès, A. Muntasar, Journal of Alloys and Compounds 438 (1–2) (2007) 131–141.
[4] F. Nie, B.C. Muddle, Scripta Materialia 37 (34) (1997) 1475–1481.
[5] B. Zberg, P.J. Uggowitzer, J.F. Löffler, Nature Materials 8 (2009) 887–891.
[6] B. Zberg, E.R. Arataa, P.J. Uggowitzera, J.F. Löffler, Acta Materialia 57 (11) (2009) 3223–3231.
[7] E. Ma, J. Xu, Nature Materials 8 (2009) 855–857.
[8] X.N. Gu, Y.F. Zheng, S.P. Zhong, T.F. Xi, J.Q. Wang, W.H. Wang, Biomaterials 31 (6) (2010) 1093–1103.
[9] R. Paris, Pub. sci. tech. ministere air (France) 45 (1934) 1–86.
[10] J.B. Clark, Transactions of the AIME 221 (1961) 644–645.
[11] J.B. Clark, Joint Committee on Powder Diffraction Standards (JCPDS) Card 12-0266, 1961.
[12] T.V. Larinova, W.W. Park, B.S. You, Scripta Materialia 45 (2001) 7–12.
[13] P.M. Jardim, G. Solorzano, J.B.V. Sande, Microscopy and Microanalysis 8 (2002) 487–496.
[14] K. Oh-ishia, R. Watanabeb, C.L. Mendisa, K. Hono, Materials Science and Engineering: A 526 (1–2) (2009) 177–184.
[15] Y.N. Zhang, D. Kevorkov, J. Li, E. Essadiqi, M. Medraj, Intermetallics 18 (12) (2010) 2402–2411.
[16] Y.N. Zhang, D. Kevorkov, F. Bridier, M. Medraj, Journal of Science and Technology of Advanced Materials 12 (2) (2011) 025003.
[17] J.B. Clark, Joint Committee on Powder Diffraction Standards (JCPDS) Card 12-0569, 1961.
[18] P. Villars, K. Cenzual, Pearson's Crystal Data – Crystal Structure Database for Inorganic Compounds (on CD-ROM), Release 2009/2010, ASM International, Materials Park, Ohio, USA.
[19] M.E. Drits, L.L. Rokhlin, V.V. Kinzhibalo, A.T. Tyvanchuk, Russian Metallurgy 6 (1985) 183–189.
[20] K.C.H. Kumar, P. Wollants, Journal of Alloys and Compounds 320 (2011) 189–198.